# Morphology control of β-SiAlON via salt-assisted combustion synthesis

*Jing Niu[1], Kazuto Harada[2], Isao Nakatsugawa[2], Tomohiro Akiyama[1#]*

*[1]Center for Advanced Research of Energy and Materials, Hokkaido University, Kita 13 Nishi 8, Kitaku, Sapporo 060-8628, Japan*

*[2]Combustion Synthesis Co., Ltd., Numazu, Shizuoka 410-0801, Japan*

[#]Corresponding author: Tel.: +81 11 706 6842; Fax: +81 11 726 0731

E-mail address: takiyama@eng.hokudai.ac.jp

**Abstract**

A facile salt-assisted combustion synthesis of β-SiAlON and systematic characterization of the endothermic effects of addition of KCl, $MgCl_2$, and $CaCl_2$ were investigated under a nitrogen pressure of 1 MPa. Single-phase products containing crystals with different shapes were obtained. The results indicated that the metal chlorides act as perfect diluents that effectively absorb the reaction heat via their melting and evaporation, which occur in the same temperature ranges as the two stages of the exothermic processes. In addition, the products exhibited different morphologies when the type or amount of metal chlorides was changed. The results of this work suggest that single-phase β-SiAlON could be fabricated with the intended morphology by simply adding different kinds of metal chlorides.

*Keywords:* Powders; Combustion synthesis; β-SiAlON; salt-assisted; microstructure

## 1. Introduction

β-SiAlON ($Si_{6-z}Al_zO_zN_{8-z}$ ($0 < z \leq 4.2$)) is an important engineering ceramic for a variety of applications because of its high strength and hardness, good thermal and chemical stability, and superior wear and thermal shock resistance [1-3]. Recently, it has been considered an excellent host material for phosphors, with potential applications for white light-emitting diodes (LEDs) because of its chemical and high-temperature stability [4-7]. Because of these outstanding properties and potential applications, β-SiAlON has been investigated extensively, especially in regard to the search for a novel low-cost synthesis route.

To date, various synthetic methods have been developed to obtain β-SiAlON products, including pressureless sintering [8], hot pressing [9], and carbothermal reduction and nitridation (CRN) [10,11]. Most of these methods, however, involve complicated equipment and processes, which limit their further applications. Combustion synthesis (CS) has been proven to be an effective energy-saving method for the synthesis of β-SiAlONs. It has many advantages over the abovementioned methods, such as simple equipment, a short reaction time, and high-purity products [12-14]. The conventional CS of β-SiAlON powders usually requires a high combustion temperature. This results in the melting and coalescence of silicon particles in the combustion front, which inhibit complete nitridation. To achieve complete conversion in the gas-solid CS of β-SiAlON, it is necessary to add a certain amount of the β-SiAlON product as a diluent to decrease the reaction heat and thus the reaction temperature. In fact, as much as 50 mass% β-SiAlON powder is needed

to obtain high-purity products [15,16]. Moreover, the post-synthesis treatment necessary to obtain a product with a fine grain size incurs high costs.

In our previous work, single-phase β-SiAlON powders with a submicron size were successfully synthesized using a small amount of NaCl as a diluent, which effectively absorbed some of the reaction heat as the latent heat of its phase transformation [17]. Furthermore, melted NaCl can be regarded as a protective shield that prevents the agglomeration of the products. Hence, fine particles are obtained. The separated particles could be easily pulverized into powders by crushing. NaCl is also considered to be a unique diluent for the synthesis of β-SiAlON because its melting point (800 ℃) and boiling point (1413 ℃) are just in the temperature ranges corresponding to the two major exothermic processes [18].

However, it was unclear whether other metal chlorides that have properties similar to NaCl could be used as diluents for the CS of β-SiAlON with a different size or shape. Therefore, the purpose of this work was to investigate the effect of metal chlorides (KCl, $MgCl_2$, and $CaCl_2$) on the synthesis of β-SiAlON and to present a detailed understanding of the endothermic processes occurring during the exothermic stages. This understanding supplies a new route for synthesizing a single-phase product with a morphology tailored by changing the type of metal chlorides to control the endothermic processes.

## 2. Experimental procedure

The starting materials used in this work were Si (purity > 99.9%, 12 μm), Al (purity > 99.9%, 14 μm), and $SiO_2$ (purity > 99.9%, 12 μm) powders, along with KCl (purity > 99.9%), $MgCl_2$ (purity > 99.9%), and $CaCl_2$ (purity > 99.9%). The effects of these different raw materials on the synthesis of β-$Si_5AlON_7$ were investigated. Different amounts of KCl, $MgCl_2$, and $CaCl_2$ were added to the raw materials as diluents. The reactant powders were mixed and mechanically activated using planetary ball milling (Gokin Planetaring Inc., Japan) at a ball-to-sample mass ratio of 10:1. The activated mixture was charged into a cylindrical carbon crucible with vents, which were used to introduce nitrogen gas. The chamber was evacuated and then filled with $N_2$ (purity: 99.999%) up to a pressure of 1 MPa. The combustion reaction was triggered by passing a current (60 A, 10 s) through a carbon foil to ignite Al powder (ignition agent) that was placed on top of the mixture. A more detailed description of the planetary milling and equipment setup for the CS was provided in a previous report [14].

Phase analyses of the products were performed using X-ray diffraction (XRD, Miniflex, Rigaku, Japan) with Cu Kα radiation (λ = 1.54056 nm). The microstructures were observed using a scanning electron microscope (FE-SEM, JSM-7400F, JEOL, Japan). The data for calculating the latent heat and theoretical adiabatic temperature ($T_{ad}$) were taken from the database in the HSC Chemistry software (Ver. 5.11, Outokumpu, Finland).

## 3. Results and discussion

### *3.1. Phase composition of the products*

Figure 1 shows the XRD patterns of the combustion-synthesized β-$Si_5AlON_7$ powders with 12 mass% of KCl, $MgCl_2$, and $CaCl_2$ added. It is clearly seen that Si peaks appear for all of the products. The unreacted Si existed because of the melting and subsequent hardening occurring under the fast reaction conditions at a high reaction temperature. In our previous work [17], when the same amount of NaCl was added, single-phase products could be obtained. The difference may be due to the different latent heats of the metal chloride phase transitions, which led to different reaction temperatures and resulted in different conversion rates for the nitridation of Si.

To determine the optimal amount of salt for obtaining complete nitridation of Si particles, a series of experiments was carried out in which varying amounts of salts were added to the raw materials. Figure 2 shows the XRD patterns of the products synthesized with the optimized amounts of additives. No Si peaks were detected for any of the samples, which indicates that the complete nitridation of the Si was achieved with these amounts of additives. In fact, the intensity of the Si peaks gradually decreased as the additive content was increased. When the proper amount of additive was provided, a single-phase product could be obtained. Taking KCl as an example, 18 mass% was found to be the proper content to obtain a product with a high purity and no trace of Si. However, with more than 18 mass%, the combustion

front flame was extinguished, and the reaction was not completed. This occurred because the reaction was not self-sustaining, since a lower amount of heat was released from the raw materials. The same results were obtained when $MgCl_2$ and $CaCl_2$ were used as the diluents, for which contents of 18 and 22 mass% were required to obtain single-phase products, respectively. The diffraction peaks were clearly observed, and they agreed with those of the standard β-SiAlON structure (JCPDS Card No. 48-1615). In addition, no metal chloride peaks were detected in the products, which indicates that their complete evaporation was achieved under the high reaction temperature.

*3.2. Change in enthalpy*

As is well known, the reaction heat from the raw materials is reduced by adding a certain amount of metal chloride. As a result, the melting and coalescence of Si particles is avoided, and the complete nitridation of Si can be achieved. Figure 3 shows the characteristics of the phase transformations of the metal chlorides in terms of the absorbed heat value $\Delta H$ (kJ/kg). The data for calculating the specific heat capacities and latent heats of the phase transformations were taken from the database in the HSC Chemistry software, Ver. 5.11. The change in the enthalpy of the raw materials during the reaction processes was estimated using $\Delta H1$ and $\Delta H2$, which correspond to the two major exothermic processes because their melting and boiling points are just in the corresponding ranges of the two-stage exothermic reaction

[17,18]. The first stage occurs at temperatures of ~660–1200 °C, and the reactions can be presented as follows:

$$Al(l) + 0.5N_2(g) \rightarrow AlN \qquad \Delta H^0 = -326.667\ kJ \qquad (1)$$

$$2Al(l) + 1.5SiO_2 \rightarrow Al_2O_3 + 1.5Si \quad \Delta H^0 = -326.775\ kJ \qquad (2)$$

The second process takes place at temperatures of ~1350–1930 °C, which includes the nitridation of Si and the simultaneous formation of β-SiAlON. This process is summarized as follows:

$$3Si + 2N_2(g) \rightarrow Si_3N_4 \qquad \Delta H^0 = -828.896\ kJ \qquad (3)$$

$$Si_3N_4 + AlN + Al_2O_3 \rightarrow \beta\text{-}SiAlON \qquad (4)$$

Therefore, the metal chlorides absorb the energy generated by reactions (1) and (2) and subsequently melt, which provides an appropriate reaction temperature for reaction (3). Because reaction (3) releases a greater amount of energy, the melted metal chlorides vaporize when they absorb it.

Figure 4 shows the changes in the enthalpy of the raw materials, which corresponds to the theoretical values of the energy absorbed in the raw materials, when the optimized amounts of KCl, $MgCl_2$, and $CaCl_2$ are added. The results from our previous work in which 12 mass% NaCl was added are also shown for comparison. It is apparent that the calculated $\Delta H1$ (kJ/kg) values are similar; that is, the reductions in the enthalpy during the first exothermic stage are almost the same for all added metal chlorides. In the second exothermic stage, the calculated values for $\Delta H2$ are also comparable, except those for the $CaCl_2$ additive, which shows a slightly higher value than the others do. In fact, in this calculation, the complete evaporation

of the salts is taken into account. However, $CaCl_2$ could not evaporate completely because of its high boiling point (1935 °C), although its peaks were not detected in the product. In our XRD analysis, we found that reducing the reaction heat was a key factor for determining the conversion rate of nitridation. These metal chlorides decreased the reaction heat by comparable amounts in two steps, in accordance with the two exothermic processes, via their melting and evaporation. The reduction in the heat released effectively prevented the Si particles of the raw materials from melting and agglomerating, which enhanced the infiltration of $N_2$. Thus, the results confirm that metal chlorides such as NaCl, KCl, and $MgCl_2$ are suitable additives for achieving single-phase β-SiAlON products.

### *3.3. Theoretical adiabatic temperatures ($T_{ad}$)*

Figure 5 shows the calculated theoretical adiabatic temperatures ($T_{ad}$) when the optimized amounts of the metal chlorides are added. For comparison, the $T_{ad}$ values in the case of NaCl addition and with no additives are also shown. Here, $T_{ad}$ was calculated using the HSC Chemistry software Ver. 5.11. The calculated $T_{ad}$ values for the different amounts of metal chlorides are also comparable, at approximately 360 °C lower than the $T_{ad}$ obtained without the salt additives. It has been reported that the product contains a large amount of unreacted Si (44 mass%) when the raw materials are used without any additives [19]. In contrast, the use of a metal chloride appropriately reduces the reaction heat, ensures a proper reaction temperature, and

thus efficiently controls the conversion of reactants to products. This theoretical calculation provides a principle for obtaining high-purity products with other, similar additives.

*3.4. Microstructure of the products*

Figure 6 shows SEM images of the β-SiAlON synthesized with 12 mass% added KCl, $MgCl_2$, and $CaCl_2$. It is obvious that the sizes and shapes of the rodlike crystals have distinctive features when different types of additives are used. The crystals have diameters of ~1 μm, lengths of ~5 μm, and round tips when KCl is added. In contrast, when $CaCl_2$ is added, the rodlike crystals are very large, with lengths of up to ~30–40 μm, diameters of ~10 μm, and regular hexagonal tips. Closer observations showed that cracks existed on the surfaces of the crystals, suggesting the incomplete growth of the crystals due to the rapid reaction rate. The crystals obtained by adding $MgCl_2$ were observed to have a shape that was between the small rod-like shapes obtained using KCl and the large shape obtained using $CaCl_2$. This large variation in the morphologies demonstrates that the additives did not have the same effect on the growth of the β-SiAlON crystals. This can be explained by the different driving forces for grain growth arising for the different chemical compositions [20].

Figure 7 shows SEM images of the β-SiAlON synthesized with the optimized amounts of the metal chlorides. The product obtained with 18 mass% KCl still consisted of rodlike crystals that were very uniform in size, with diameters of 0.5 μm

and lengths of 5 μm, although they were smaller than those obtained when 12 mass% KCl was added (see Fig. 6(a)). However, the crystals developed into small particles for the higher $MgCl_2$ and $CaCl_2$ contents, in contrast to the structures shown in Figs. 6(b) and (c), respectively. These distinct changes in morphology were mainly caused by the different reaction temperatures. At a higher temperature, the mass transport will be enhanced, and morphology evolution of the β-SiAlON grains will tend to occur more easily. Therefore, at a higher temperature, or with the addition of a smaller quantity of the additive, a dynamic ripening mechanism will allow the rapid growth of coarse rodlike crystals. In contrast, at a lower temperature, or with the addition of a larger quantity of the additive, the grain growth will be greatly restricted. Figure 8 displays a series of SEM images showing the morphology evolution of samples produced using $CaCl_2$ as the diluent. These images support the aforementioned statement that the growth of the crystals is controlled by the reaction temperature. They also indicate that the dimensions of the crystal structure change during its evolution, with a reduction in the diameter of the rodlike structures and an increase in their length. These dimensional changes occur because the discontinuity of the rough surface morphology leads to evolution into an equilibrium crystal shape with the minimum total surface energy. There are some large rodlike crystals with concave tips, as shown in Fig. 8(d). The formation of this concave tip shape for rodlike β-SiAlON is discussed in detail by Liu et al. [21].

Briefly, for the different kinds of additives, the morphology of the crystals is affected by the different chemical compositions and the different driving forces. For

the same type of additives, the morphology of the crystals is controlled by the reaction temperature. These results will be helpful for designing the morphology of β-SiAlON crystals.

## 4. Conclusions

Single-phase β-SiAlON products with different morphologies were obtained by adding different amounts of KCl, $MgCl_2$, and $CaCl_2$ to the raw materials. The metal chlorides were considered to be suitable additives for the synthesis of single-phase β-SiAlON for the following reasons. First, their melting absorbed the energy of the first exothermic process, and their evaporation absorbed that of the second exothermic process. Thus, the latent heat of their phase transitions could control the reaction heat and ensure an appropriate reaction temperature, which promoted the complete nitridation of Si. On the other hand, the morphology of the product was strongly affected by the type of chloride: the size of the rodlike crystals became smaller with increasing KCl content, while the coarse rodlike crystals developed into small particles when the amount of $MgCl_2$ or $CaCl_2$ was increased. These findings prove that this is a novel and facile method for fabricating single-phase β-SiAlON crystals with a tailored morphology by changing the type or amount of metal chlorides.

## Acknowledgements

The authors wish to thank Dr. Sakurai of Combustion Synthesis Co., Ltd. for valuable discussions.

**References**


[1] K.H. Jack, Sialons and related nitrogen ceramics, J. Mater. Sci. 11 (1976) 1135-1158.

[2] T. Ekström, P.O. Käll, M. Nygren, P.O. Olssen, Dense single-phase β-SiAlON ceramics by glass-encapsulated hot isostatic pressing, J. Mater. Sci. 24 (1989) 1853-1861.

[3] T. Ekström, M. Nygren, SiAlON ceramics, J. Am. Ceram. Soc. 75[2] (1992) 259-276.

[4] R.-J. Xie, N. Hirosaki, H.-L. Li, Y.Q. Li, M. Mitomo, Synthesis and photoluminescence properties of β-SiAlON:$Eu^{2+}$($Si_{6-z}$ $Al_zO_zN_{8-z}$:$Eu^{2+}$): A promising green oxynitride phosphor for white light-emitting diodes, J. Electrochem. Soc. 154 (2007) J314-J319.

[5] T.-C. Liu, B.-M. Cheng, S.-F. Hu, R.-S. Liu, Highly stable red oxynitride β-SiAlON:$Pr^{3+}$ phosphor for light-emitting diodes, Chem. Mater. 23 (2011) 3698-3705.

[6] J. Niu, G. Saito, T. Akiyama, A new route to synthesize β-SiAlON:$Eu^{2+}$ phosphors for white light-emitting diodes, APEX 6 (2013) 042105.

[7] J.H. Chung, J.H. Ryu, Photoluminescence and LED application of beta-SiAlON:$Eu^{2+}$ green phosphor, Ceram. Inter. 38 (2012) 4601-4606.

[8] C. Zhang, R. Janssen, N. Claussen, Pressureless sintering of β-SiAlON with improved green strength by using metallic Al powder, Mater. Lett. 57 (2003) 3352-3356.

[9] S.-L. Hwang, I.-W. Chen, Reaction hot pressing of α′- and β′-SiAlON ceramics, J. Am. Ceram. Soc. 77 [1] (1994) 165-171.

[10] K.J.D. MacKenzie, D.V. Barneveld, Carbothermal synthesis of β-SiAlON from mechanochemically activated precursors, J. Eur. Ceram. Soc. 26 (2006) 209-215.

[11] J. Li, H. Ma, Q. Fang, Synthesis of prismatic beta-sialon from the precursor of SBA-15 incorporated with $Al(NO_3)_3$ via carbothermal reduction nitridation, Ceram. Inter. 34 (2008) 1791-1795.

[12] M. Hiramoto, N. Okinaka, T. Akiyama, Self-propagating high-temperature synthesis of nonstoichiometric wüstite, J. Alloy. Comp. 520 (2012) 59-64.

[13] R. Sivakumar, K. Aoyagi, T. Akiyama, Thermal conductivity of combustion synthesized beta-SiAlONS, Ceram. Inter. 35 (2009) 1391-1395.

[14] K. Aoyagi, T. Hiraki, R. Sivakumar, T. Watanabe, T. Akiyama, Mechanically activated combustion synthesis of β-$Si_{6-z}Al_zO_zN_{8-z}$ (z=1–4), J. Am. Ceram. Soc. 90 (2007) 626-628.

[15] X. Yi, K. Watanabe, T. Akiyama, Fabrication of dense β-SiAlON by a combination of combustion synthesis (CS) and spark plasma sintering (SPS), Intermetallics 18 (2010) 536-541.

[16] M. Shahien, M. Radwan, S. Kirihara, Y. Miyamoto, T. Sakurai, Combustion synthesis of single-phase β-sialons (z = 2-4), J. Eur. Ceram. Soc. 30 (2010) 1925-1930.

[17] J. Niu, X. Yi, I. Nakatsugawa, T. Akiyama, Salt-assisted combustion synthesis of β-SiAlON fine powders, Intermetallics 35 (2013) 53-59.

[18] X. Yi, J. Niu, T. Nakamura, T. Akiyama, Reaction mechanism for combustion synthesis of β-SiAlON by using Si, Al, and $SiO_2$ as raw materials, J. Alloy. Comp. 561 (2013) 1-4.

[19] K. Aoyagi, R. Sivakumar, X. Yi, T. Watanabe, T. Akiyama, Effect of diluents on high purity beta-SiAlONs by mechanically activated combustion synthesis, J. Ceram. Soc. Japan 117 (2009) 777-779.

[20] G. Liu, C. Pereira, K. Chen, H. Zhou, X. Ning, J.M.F. Ferreira, Fabrication of one-dimensional rod-like [alpha]-SiAlON powders in large scales by combustion synthesis, J. Alloy. Comp. 454 (2008) 476-482.

[21] G. Liu, K. Chen, J. Li, Growth mechanism of crystalline SiAlON microtubes prepared by combustion synthesis, CrystEngComm 14 (2012) 5585-5588.

**Figure captions**

**Fig. 1** XRD patterns of combustion-synthesized β-SiAlON (z = 1) obtained with the addition of 12 mass% KCl, $MgCl_2$, or $CaCl_2$ (this work) or the addition of 12 mass% NaCl (previous work).

**Fig. 2** XRD patterns of combustion-synthesized β-SiAlON (z = 1) obtained with optimized amounts of KCl, $MgCl_2$, and $CaCl_2$ (mass%).

**Fig. 3** Characteristics of phase transformations of metal chlorides and changes in heat $\Delta H$ (kJ/kg).

**Fig. 4** Change in enthalpy of the raw materials ($\Delta H$, kJ/kg) for the addition of optimized amounts of KCl (18 mass%), $MgCl_2$ (18 mass%), and $CaCl_2$ (22 mass%), along with $\Delta H$ for NaCl is listed here, which were calculated from their absorbed heat values corresponding to the two exothermic processes.

**Fig. 5** Calculated adiabatic temperatures ($T_{ad}$) for the addition of optimized amounts of KCl (18 mass%), $MgCl_2$ (18 mass%), and $CaCl_2$ (22 mass%), along with $T_{ad}$ for addition of 12 mass% NaCl (previous work) and that obtained when no additives were used. These results were calculated according to the absorbed heat values.

**Fig. 6** SEM images of combustion-synthesized β-SiAlON powders obtained with 12 mass% (a) KCl, (b) $MgCl_2$, and (c) $CaCl_2$. (d) Enlarged image of the area enclosed in a square in (c).

**Fig. 7** SEM images of combustion-synthesized β-SiAlON powders obtained using optimized amounts of (a) KCl (18 mass%), (b) $MgCl_2$ (18 mass%), and (c) $CaCl_2$ (22 mass%).

**Fig. 8** SEM images of combustion-synthesized β-SiAlON powders obtained using (a,b) 22 mass% $CaCl_2$ and (c–f) 12 mass% $CaCl_2$.

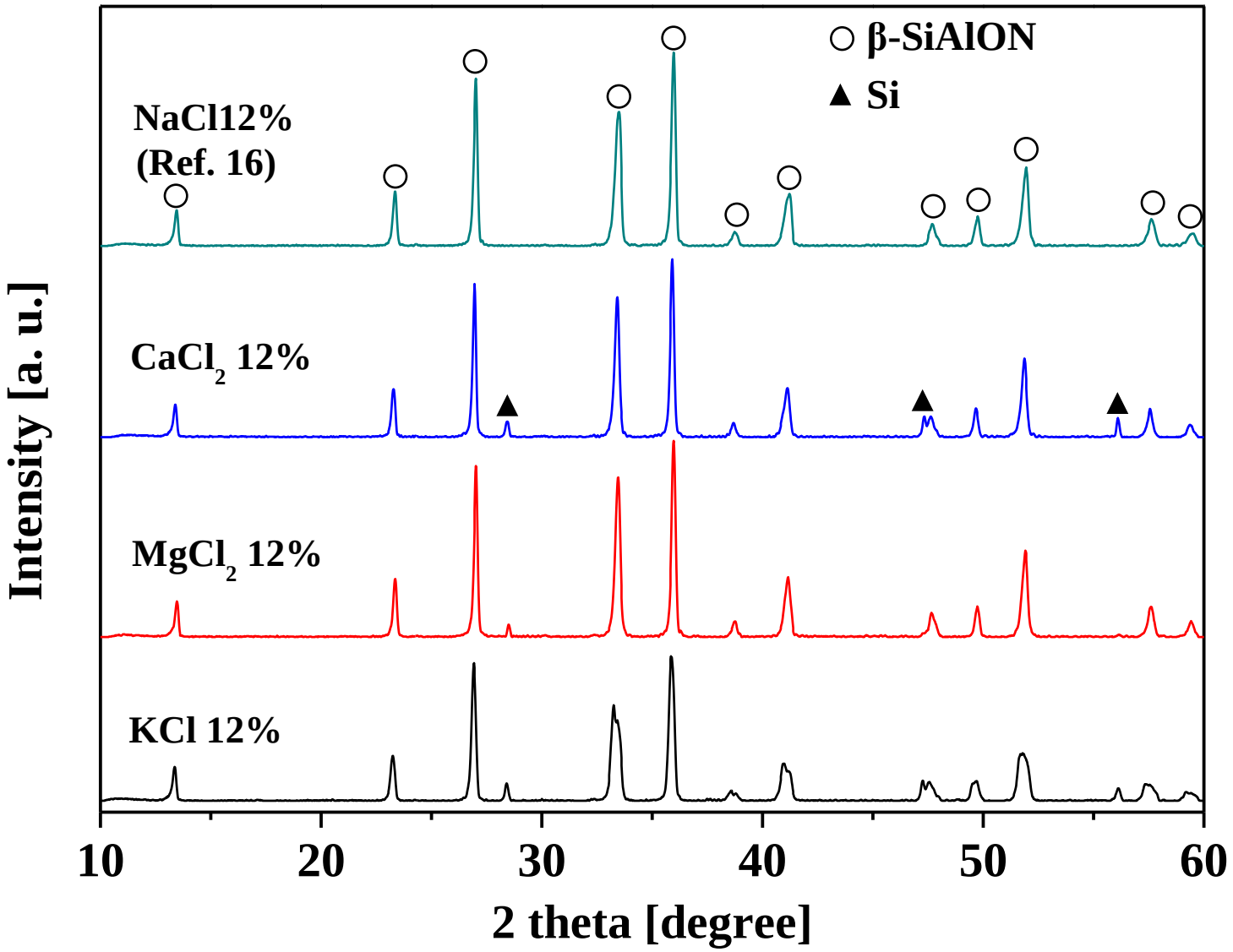


**Fig. 1** XRD patterns of combustion-synthesized β-SiAlON (z = 1) obtained with the addition of 12 mass% KCl, $MgCl_2$, or $CaCl_2$ (this work), or the addition of 12 mass% NaCl (previous work).

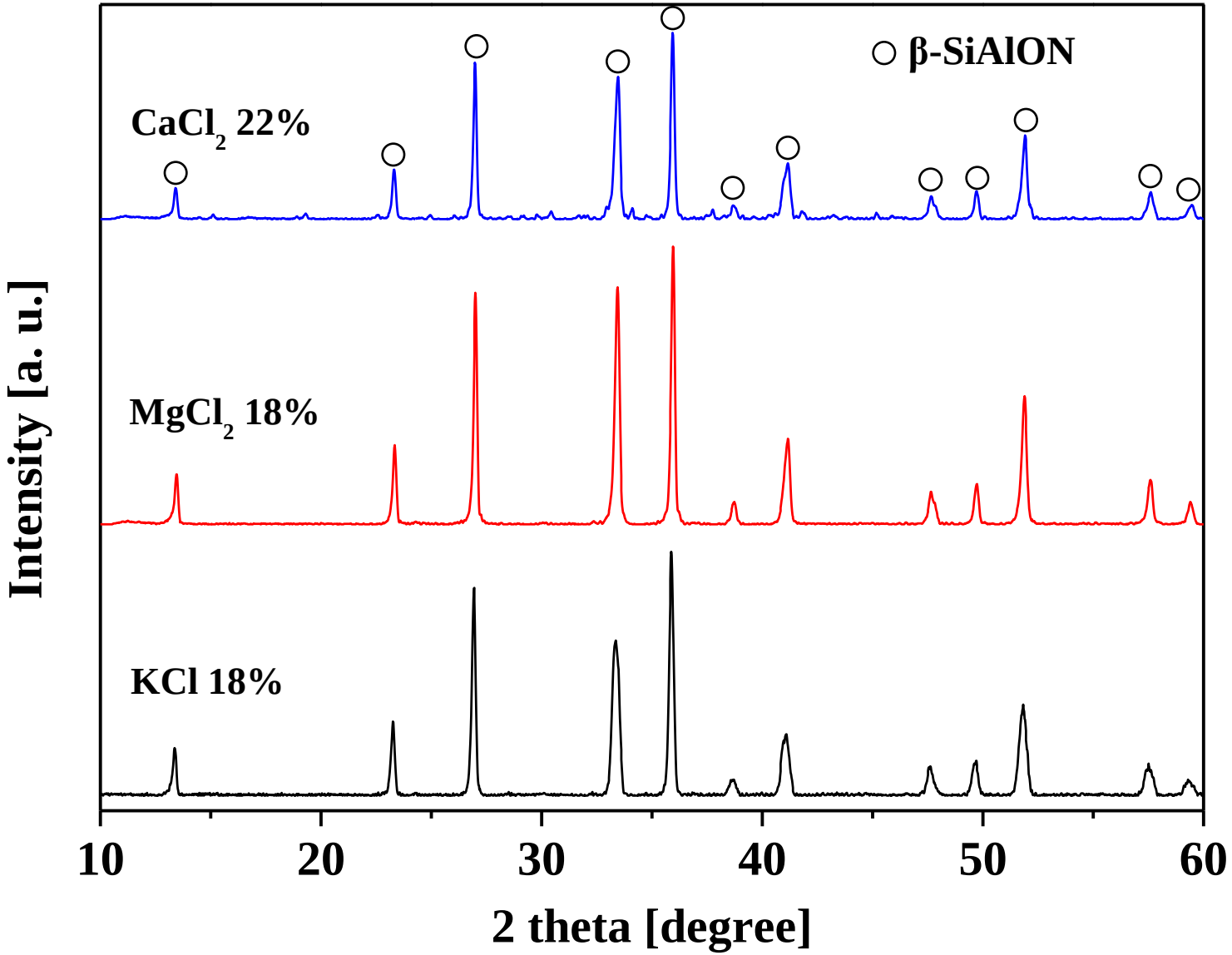


**Fig. 2** XRD patterns of combustion-synthesized β-SiAlON (z = 1) obtained with optimized amounts of KCl, $MgCl_2$, and $CaCl_2$ (mass%).

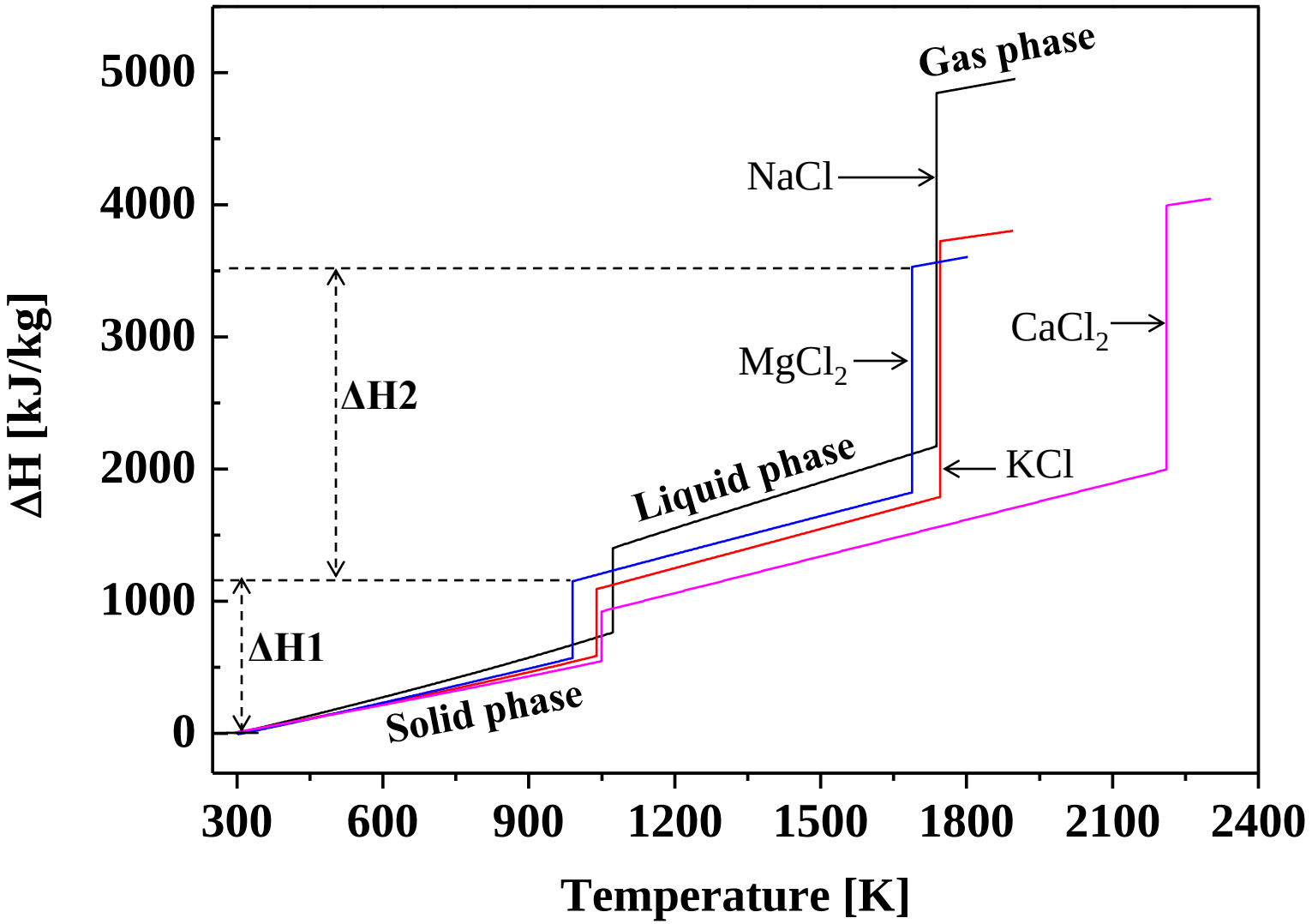


**Fig. 3** Characteristics of phase transformations of metal chlorides and changes in heat *ΔH* (*kJ/kg*).

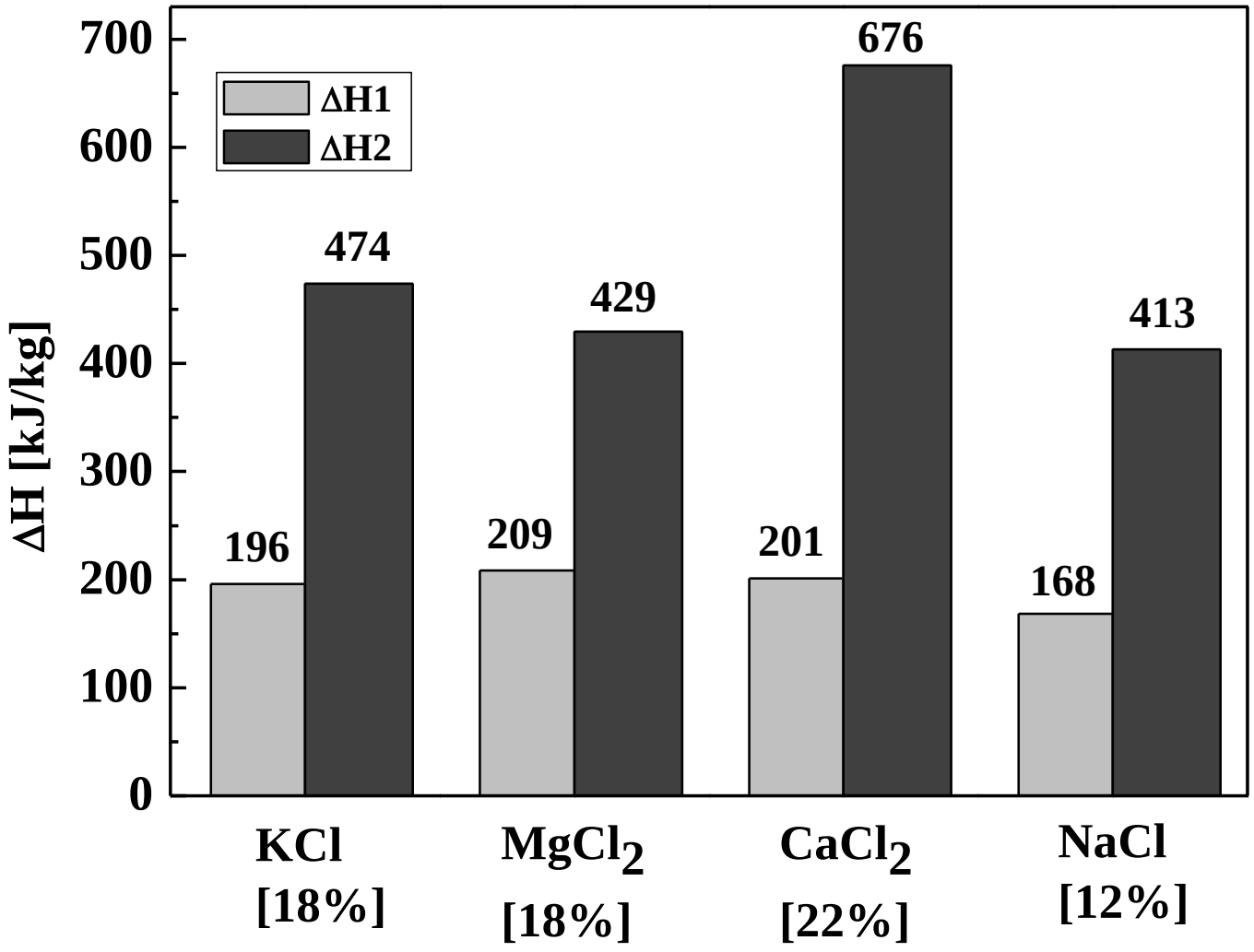


**Fig. 4** Change in enthalpy of raw materials (*ΔH*, *kJ/kg*) for the addition of optimized amounts of KCl (18 mass%), $MgCl_2$ (18 mass%), and $CaCl_2$ (22 mass%), along with *ΔH* for NaCl is listed here, which were calculated from their absorbed heat values corresponding to the two exothermic processes.

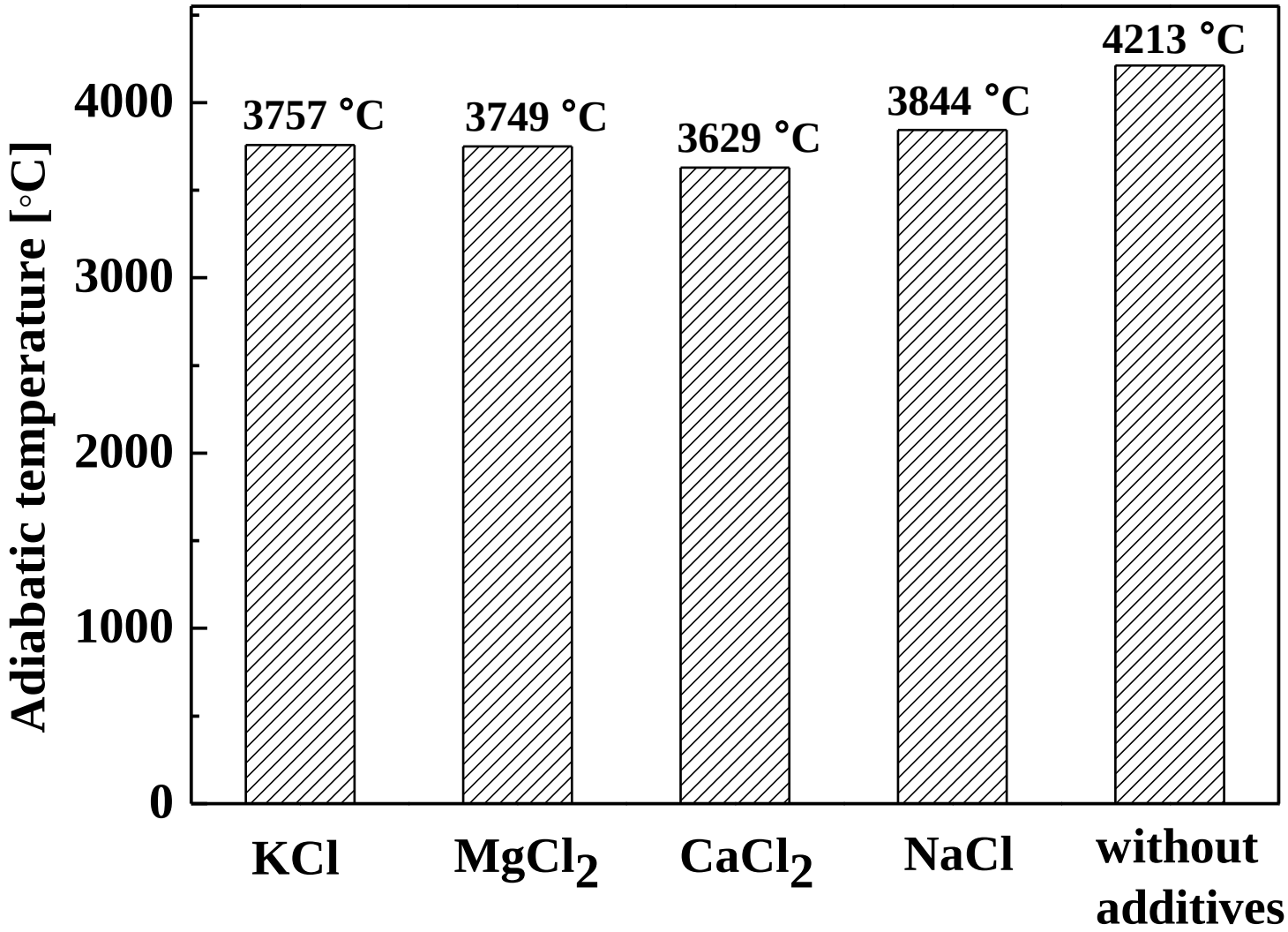


**Fig. 5** Calculated adiabatic temperatures ($T_{ad}$) for the addition of optimized amounts of KCl (18 mass%), $MgCl_2$ (18 mass%), and $CaCl_2$ (22 mass%), along with $T_{ad}$ for addition of 12 mass% NaCl (previous work) and that obtained when no additives were used. These results were calculated according to the absorbed heat values.

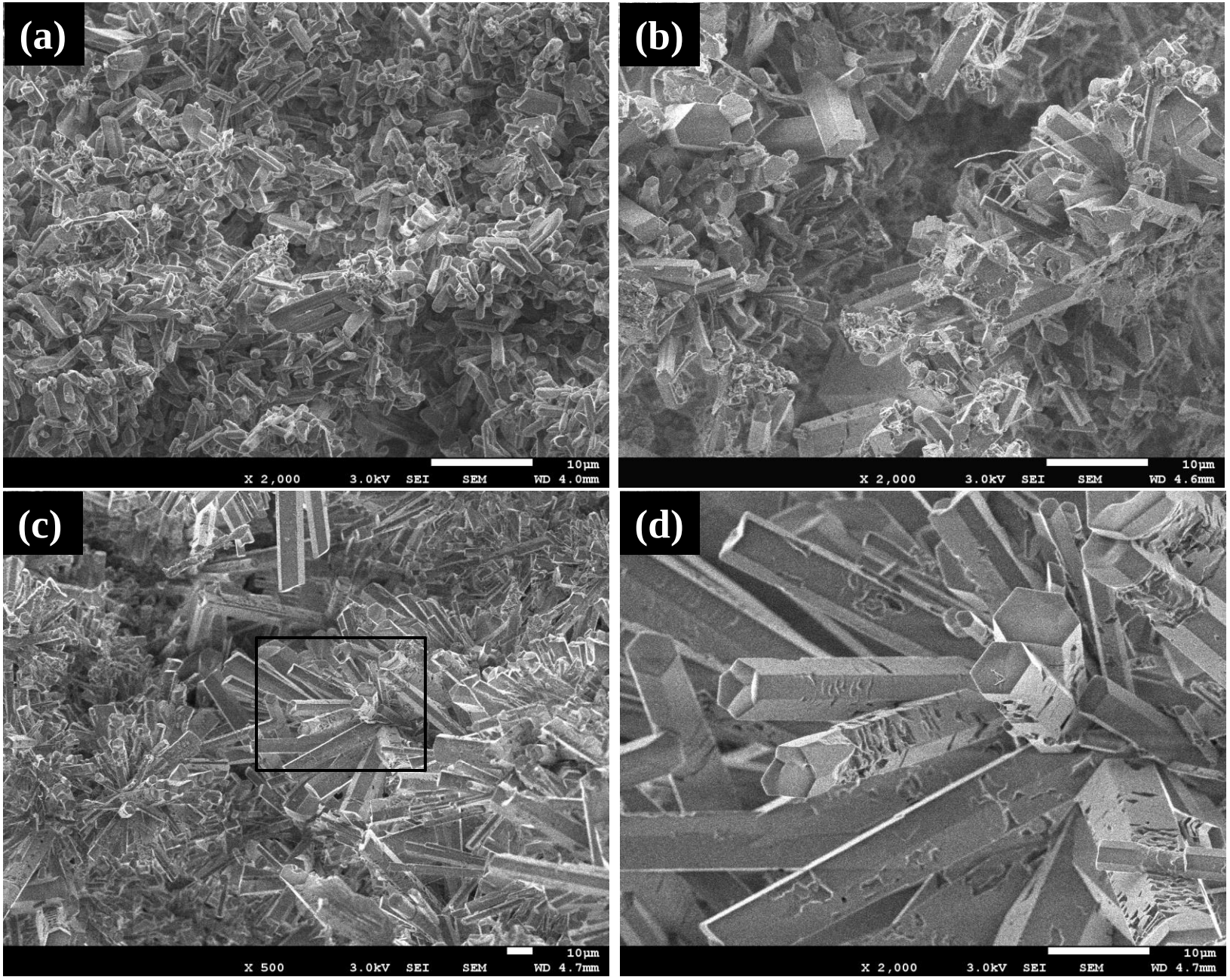


**Fig. 6** SEM images of combustion-synthesized β-SiAlON powders obtained with 12 mass% (a) KCl, (b) $MgCl_2$, and (c) $CaCl_2$. (d) Enlarged image of the area enclosed in a square in (c).

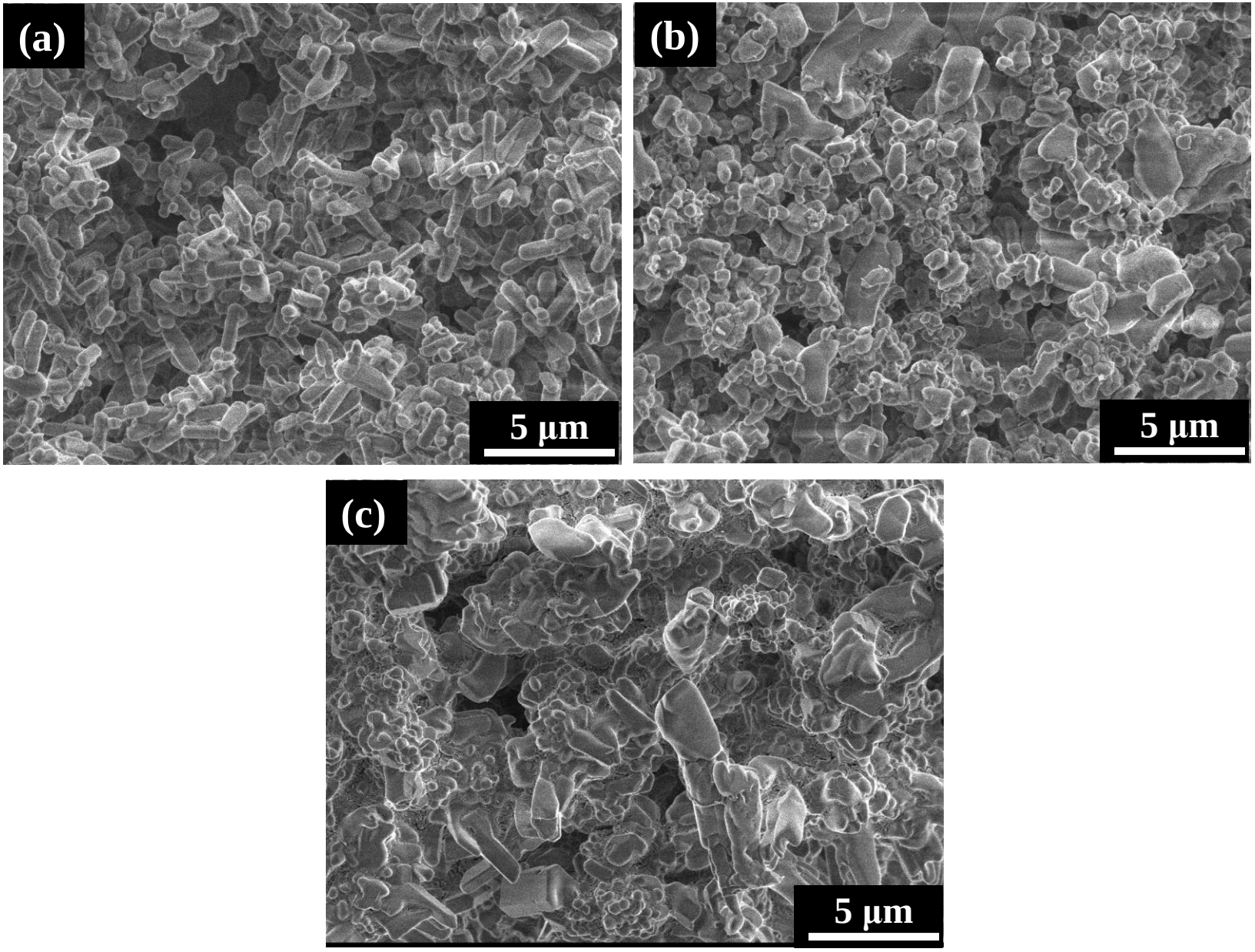


**Fig. 7** SEM images of combustion-synthesized β-SiAlON powders obtained using optimized amounts of (a) KCl (18 mass%), (b) $MgCl_2$ (18 mass%), and (c) $CaCl_2$ (22 mass%).

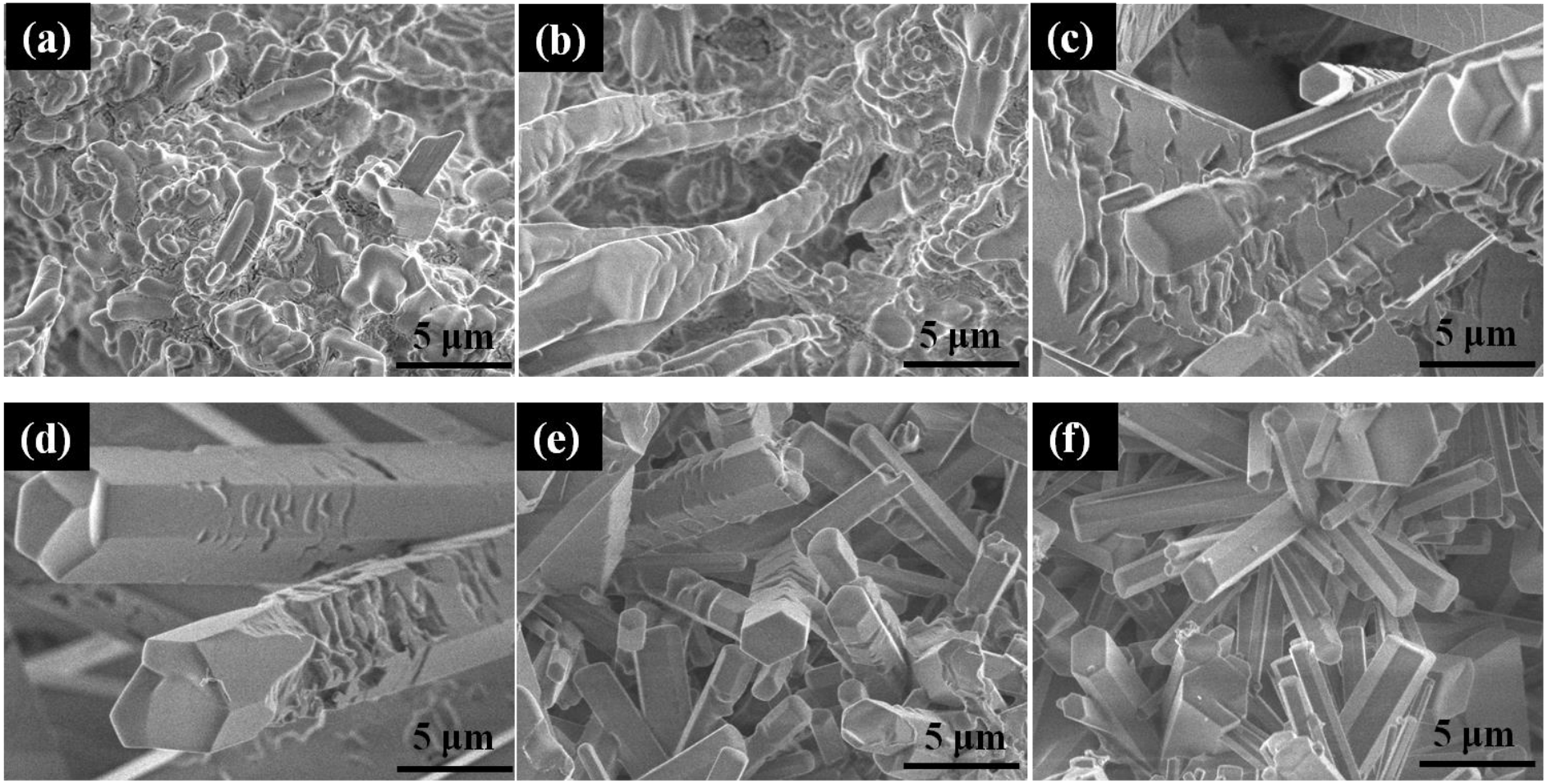


**Fig. 8** SEM images of combustion-synthesized β-SiAlON powders obtained using (a, b) 22 mass% $CaCl_2$ and (c-f) 12 mass% $CaCl_2$.